Hydrol. Earth Syst. Sci. Discuss., 12, 671–704, 2015
www.hydrol-earth-syst-sci-discuss.net/12/671/2015/
doi:10.5194/hessd-12-671-2015

Hydrology and Earth System Sciences
Discussions

Precipitation in the Amazon and its relationship with moisture transport and tropical Pacific and Atlantic SST from the CMIP5 simulation

G. Martins[1], C. von Randow[1], G. Sampaio[1], and A. J. Dolman[2]

[1]Earth System Science Center/National Institute for Space Research, Sao Paulo, Brazil
[2]Department of Earth Sciences/Vrije Universiteit Amsterdam, Amsterdam, the Netherlands

Received: 12 December 2014 – Accepted: 21 December 2014 – Published: 15 January 2015

Correspondence to: G. Martins (guilherme.martins@inpe.br)

Published by Copernicus Publications on behalf of the European Geosciences Union.

Abstract

Studies on numerical modeling in Amazonia show that the models fail to capture important aspects of climate variability in this region and it is important to understand the reasons that cause this drawback. Here, we study how the general circulation models of the Coupled Model Intercomparison Project Phase 5 (CMIP5) simulate the inter-relations between regional precipitation, moisture convergence and Sea Surface Temperature (SST) in the adjacent oceans, to assess how flaws in the representation of these processes can translate into biases in simulated rainfall in Amazonia. Using observational data (GPCP, CMAP, ERSST.v3, ERAI and evapotranspiration) and 21 numerical simulations from CMIP5 during the present climate (1979–2005) in June, July and August (JJA) and December, January and February (DJF), respectively, to represent dry and wet season characteristics, we evaluate how the models simulate precipitation, moisture transport and convergence, and pressure velocity (omega) in different regions of Amazonia. Thus, it is possible to identify areas of Amazonia that are more or less influenced by adjacent ocean SSTs. Our results showed that most of the CMIP5 models have poor skill in adequately representing the observed data. The regional analysis of the variables used showed that the underestimation in the dry season (JJA) was twice in relation to rainy season as quantified by the Standard Error of the Mean (SEM). It was found that Atlantic and Pacific SSTs modulate the northern sector of Amazonia during JJA, while in DJF Pacific SST only influences the eastern sector of the region. The analysis of moisture transport in JJA showed that moisture preferentially enters Amazonia via its eastern edge. In DJF this occurs both via its northern and eastern edge. The moisture balance is always positive, which indicates that Amazonia is a source of moisture to the atmosphere. Additionally, our results showed that during DJF the simulations in northeast sector of Amazonia have a strong bias in precipitation and an underestimation of moisture convergence due to the higher influence of biases in the Pacific SST. During JJA, a strong precipitation bias was observed in the southwest sector associated, also with a negative bias of mois-

ture convergence, but with weaker influence of SSTs of adjacent oceans. The poor representation of precipitation-producing systems in Amazonia by the models and the difficulty of adequately representing the variability of SSTs in the Pacific and Atlantic oceans may be responsible for these underestimates in Amazonia.

1 Introduction

The Amazon river basin is the largest in the world accounting for 20 % of the fresh water on the planet while the rainforest is responsible for approximately 10 % of land productivity and biomass (Joetzjer et al., 2013). It is also one of the regions with strongest convective activity on the globe, playing an important role in the general atmospheric circulation (Andreoli et al., 2012). In fact, the region plays a key role in global climate by regulating the water and carbon cycles (Foley, 2002; Yoon and Zeng, 2010).

The Amazon region exhibits a well-marked annual variability of rainfall characterized by summers with abundant rainfall in the whole region and winters with precipitation localized in north and west (Ronchail et al., 2002). This is because the precipitation is modulated by the meridional displacement of the Intertropical Convergence Zone (ITCZ) following the dynamics of the tropical atmospheric circulation (Cook et al., 2012) and the inter-hemispheric Sea Surface Temperature (SST) gradient in the tropical Atlantic (Kousky et al., 1984; Aceituno, 1988; Marengo et al., 2011, 2012) and also the SST in the tropical Pacific.

Changes in the meridional gradient of SST in the tropical Atlantic may influence precipitation in the Amazon dry season by changing the pattern of moisture convergence and vertical motion (Good et al., 2008). The seasonality of precipitation is dominated by north–south migration of the precipitation band influenced by trade winds (Xie and Carton, 2004), and the SST can influence this seasonality through its temporal fluctuations.

Strong upward movement over South America is considered important part of the circulation of the Walker cell (Kousky, 1984). It is known that anomalous subsidence

(uplift) on the Central Pacific induced by cooling (heating) over the central equatorial Pacific can change the east–west circulation associated with the Walker cell resulting in an increase (decrease) in precipitation over tropical South America. Numerical studies (Harris et al., 2008) during the boreal summer coinciding with the dry season in the Amazon showed that heating (cooling) in the Tropical North Atlantic (South) can cause drought events over the Amazon. Projections of available earth system models feature a wide spread in rainfall over the Amazon, suggesting that some aspect associated with the dynamics of rainfall in the region are not well represented by these models (Yin et al., 2013). The rainfall in this region is an important component because it directly influences the hydrological cycle and carbon balance, therefore, it is important to understand what dynamics or other factors that cause the high variability between models.

This study aims to assess the causes of the CMIP5 models failures to represent the Amazon rainfall (Joetzer et al., 2013; Yin et al., 2013), and their relation to sea surface temperature patterns in the adjacent oceans and regional moisture transport.

2 Data and methodology

2.1 Observed datasets

The observed data are from the Global Precipitation Climatology Project (GPCP, Huffman et al., 1997) and the CPC Merged Analysis of Precipitation (CMAP) for the precipitation (PREC) for the period 1979–2005.

The GPCP is a product of global precipitation from the World Climate Research Programme (WRCP) available from 1979, with spatial resolution of $2.5^{\circ} \times 2.5^{\circ}$ (lat × lon) and monthly temporal resolution, with the objective of improving understanding of its spatial and temporal pattern around the globe. The CMAP is also a monthly precipitation analysis product available from 1979 in the resolution of $2.5^{\circ} \times 2.5^{\circ}$ (lat × lon) formed by combining data from various ground stations combined with satellite esti-

mates of precipitation, as well as algorithms (Xie and Arkin, 1997). These two data sets were selected because they represent satisfactorily the distribution of rainfall in Amazonia as shown by Pinto et al. (2009).

We also use the Extended Reconstructed Sea Surface Temperature version 3 dataset (ERSST.v3, Smith et al., 2008) consisting of monthly data from buoys and ships around the globe. These data are available from 1854 on resolution of 2.0° × 2.0° (lat × lon) and we rescaled the SST to the 2.5° × 2.5° (lat × lon).

Monthly variables of zonal (v) and meridional (u) wind, specific humidity (q) and surface pressure (psfc) were obtained from the European Centre for Medium-Range Weather Forecasts (ECMWF) Interim Reanalysis (ERAI; Dee et al., 2011). These variables are used to calculate the vertically integrated moisture flux on each edge of the domain of Fig. 1 (box 1, 2, 3 and 4 and gray box) and have a spatial resolution of 1.5° × 1.5° (lat × lon). ERAI has been demonstrated to be able to capture the ITCZ compared with observations, and is the best among three state-of-art reanalysis products for the Amazonian (Lorenz and Kunstmann, 2012). For this work, the ECMWF data were also interpolated to 2.5° × 2.5° (lat × lon) resolution.

Finally, monthly evapotranspiration (evap, Mueller et al., 2013) data were obtained from an ensemble of various estimates, such as surface measurements, satellite and surface models comprising the period of 1989–2005.

2.2 Model outputs

We use numerical simulations of the suite of General Circulation Models of the Atmosphere Coupled Model Intercomparison Project Phase 5 (CMIP5, Taylor et al., 2012). Information about the models and their characteristics is presented in Table 1. The period used for the analysis is the historical period for the years 1979–2005, which represents the present climate and is a period where observational records are more reliable and available. The selected variables are the same as the observed data listed in the previous section, that is, SST, PREC, u, v, q, psfc and evap. Since the models

do not exhibit the same spatial resolution of the observed data, each model output was interpolated to 2.5° × 2.5° (lat × lon) resolution.

2.3 Study area

The analysis uses four boxes over the Amazon (Fig. 1) with the following dimensions: Box1 (7.5° S–0° and 75–60° W), Box2 (15.0–7.5° S and 75–60° W), Box3 (10.0–2.5° S and 60–45° W) and Box4 (2.5° S–5.0° N and 60–45° W). The four boxes are selected in this configuration because the Amazon rainfall distribution is very irregular (Zeng, 1999). Three other boxes are selected over the oceans, one over the North Atlantic (NAT, 6.0–22.0° N and 80–15° W), one over South Atlantic (SAT, 25.0° S–2.0° N and 35° W–10° E) and the NINO3.4 region in the Pacific (5.0° S–5.0° N and 170° W–120° W).

The vertically integrated moisture flux is calculated for box 1, 2, 3 and 4 and for the gray box shown in Fig. 1.

2.4 Correlation and vertically integrated moisture flux

For the analyses of influence of SST, moisture transport and precipitation in the Amazon, we extracted the time series of precipitation averaged over each box in the Amazon, and calculated its correlation (r, Eq. 1) to the SST in the ocean areas shown in Fig. 1, for the period 1979–2005.

$$r = \frac{C_{x,y}}{S_x S_y} \tag{1}$$

where $C_{x,y}$ is the covariance between x and y, and $S_x S_y$ represent the SD. Correlation coefficients are calculated here between the SST for the months of May or November and precipitation averages from June through August (JJA) or December through February (DJF). The purpose of relating SST to lagged precipitation is to consider the effect of atmospheric memory of this teleconnection.

The transport of water vapor (Q) is calculated according to Rao et al. (1996) for the four boxes on Amazon. The purpose of this calculation is to evaluate the transport entering (plus transport) or out (negative transport) the edges of the selected domain. The calculation follows the equations:

$$Q_v = \frac{1}{g}\int_{pt}^{po}(qv)\,\mathrm{d}p \tag{2}$$

$$Q_u = \frac{1}{g}\int_{pt}^{po}(qu)\,\mathrm{d}p \tag{3}$$

Where Q_u and Q_v flows are moisture zonal and meridional, respectively, g ($\mathrm{m\,s^{-2}}$) is the acceleration due to gravity, q ($\mathrm{kg\,kg^{-1}}$) is the specific humidity, u ($\mathrm{m\,s^{-1}}$) and v ($\mathrm{m\,s^{-1}}$) are the zonal and meridional components of the winds and p_t and p_o represent the pressure (hPa) at 300 hPa and the surface, respectively. The unit flows are given in in $\mathrm{mm\,day^{-1}}$.

To perform the calculation in the east, west, north and south edges should be set in each of these edges the limits of boundaries according to Eqs. (4) and (5) proposed by Lima et al. (2010).

$$Q_j = \int_{lat1}^{lat0} Q_i\,\mathrm{d}y \tag{4}$$

$$Q_k = \int_{lon1}^{lon0} Q_i\,\mathrm{d}x \tag{5}$$

The calculation is done on the edges using the above equations where it is necessary to fix the latitude and longitude borders. The index j (Eq. 4) defines the longitude to

fix the east or west borders, lat1 (lat) border represents the latitude value at the south (north) edge. The index i in the equations represents the vertically integrated moisture flux calculated previously. The index k (Eq. 5) defines the latitude to fix the north or south borders, lon1 (lon) is the longitude on the western (east) edge.

To calculate the bias of each model relative to the observed data from GPCP and ERAI, we use the Eq. (6). This calculation is applied to the values of precipitation and moisture convergence. This calculation gives us a good indication of the bias of the models in reproducing the observation.

$$\% = \left[\frac{(\text{model} - \text{observation})}{\text{observation}}\right] \times 100 \tag{6}$$

3 Results

Figure 2 shows the average monthly precipitation (Fig. 2a), evapotranspiration (Fig. 2b) and moisture convergence (Fig. 2c) for all models compared to observations or reanalysis, corresponding to spatial and temporal averages in the gray box of Fig. 1. Observations are presented in a thick red line, with a pink shaded region representing their monthly SD, and model simulations are the different colored lines.

All the models are able to represent the seasonality of precipitation with rainy summer (DJF) and dry winter (JJA) conditions in the Southern Hemisphere (Marengo et al., 2012), but the intensity is underestimated throughout the year, especially during the dry season (JJA). In JJA some models produce close to zero rainfall. Some models represent satisfactorily the seasonality, for instance ACCESS1-0, HADGEM2-CC-ES HADGEM2 NMI-CM4 and MRI-CGCM3. The results found here are similar to those obtained by Joetzjer et al. (2013) who evaluated the Amazon rainfall of these climate models. In that work, it was shown that the models underestimate the dry period precipitation despite the improvement in spatial resolution compared to previous versions of the models.

Evaporation represents an important local moisture source to the atmosphere. In Fig. 2b, the evapotranspiration simulated by most models shows an overestimation compared to the mean of a set of evaporation estimates (Mueller et al., 2013). However, some models (BCC-CSM1.1, CANESM2 and FGOALS-G2) show underestimation in the dry season (JJA). Other models are out of phase in relation to that seen in the observation in this period, for instance MRI-CGCM3 and GFDL-ESM2G. They present minimum values in the August, September and October quarter. Despite this overestimation, we note that the models are generally able to represent well the seasonality of this variable, showing maxima during the rainy season and minima in the dry season consistent with that observed in precipitation (Fig. 2a). The convergence of vertically integrated moisture (Fig. 2c) shows high variability among the models in the rainy season but in the dry season, most of them tend to underestimate the moisture convergence.

To compare the performance of the models in relation to the observed data (GPCP) we plot in Fig. 3 the correlation between the observation and the model in relation to root-mean-square (RMS) as defined by the standard model (σ model) normalized by observation (σ observation) during JJA (blue dot) and DJF (red dot) in the period 1979–2005 for precipitation in the gray box of Fig. 1. Some models show negative correlations (BCC-CSM1.1, CNRM-CM5, GFDL-CM3, MIROC-ESM, MPI-ESM-LR, MRI-CGCM3 and NORESM1-M) and for simplicity and visualization of the results, they are not shown in the diagram. Most of the models have low correlations, varying between 0.3 and 0.6 for both seasons. However, the models that show the best correlations (above 0.6) are those of the quarter JJA, that is, for the IPSL-CM5A-LR, IPSL-CM5A-MR, CCSM4 and HADGEM2-ES models. The low normalized SD of the models shows that most models are not able to represent the pattern of variability of the observed data. The RMS for most models is high, with values above 3.5 and it shows that the models have poor ability to simulate the observed data. In general, the CMIP5 models are unable to satisfactorily represent the relationship between the observed and simulated rainfall in the Amazon in the present climate.

The percentage bias of the modeled precipitation (Eq. 6) in Amazonia (gray box in Fig. 1) is compared to GPCP during the dry (JJA, gray bar) and rainy season (DJF, white bar) in the period 1979–2005 in Fig. 4. Beside bias, the average of all models (Mean) and standard error of the mean of all models (SEM) is shown. Positive or negative bias indicates overestimation or underestimation, respectively.

We note a pattern of underestimates in most models compared to the observed data from GPCP in the four boxes for both the dry and rainy season. Consistently, Fig. 5 presents bias of simulated pressure velocity omega ($\mathrm{Pa\,s^{-1}}$) at 500 hPa that shows that most models underestimate the convection in comparison to ERAI, and the result is an inhibition of simulated upward movements, which in turn, suppresses the formation of precipitation.

However, there is a small set of models that presents overestimation, for instance ACCESS1-0, GISS-E2-R, HADGEM-CC, HADGEM-ES and INM-CM4. The spatial pattern of the bias of precipitation shows that these models exhibit overestimation of precipitation, mainly in box 2 during the dry period consistent with the bias of simulated pressure velocity omega ($\mathrm{Pa\,s^{-1}}$) at 500 hPa. It is also shown that the positive bias of precipitation is greater in the region of the ITCZ of the Atlantic and tropical Pacific Oceans. The negative bias of precipitation is observed for the Amazon.

It is also interesting to note that, in box 3, during the wet season, there is a positive bias in simulation of vertical motions (Fig. 5), which may partly explain the lower biases in precipitation simulations in that area.

During JJA, box 3 (Eq. 2) is the area that shows the smallest underestimation (overestimation) on average, that is, 51 % (13 %). During the rainy season, box 3 (Eq. 2) presents an overestimation (underestimation) of 1 % (41 %). On average, rainfall in the dry season is underestimated by approximately 38 % (mean values of box 1, 2, 3 and 4), but in the rainy season, this underestimation is 21 %.

The mean SEM of the four boxes in the dry season (rainy) is 9.3 (5.0) $\mathrm{mm\,day^{-1}}$, that is, the models underestimate more in the dry season than in the rainy season. Cook et al. (2012) analyzed 24 models of the Fourth Assessment Report (AR4) in order to

assess the factors responsible for changes in rainfall in the Amazon in response to climate change. The results showed that most models showed a significant decrease of approximately 10.5 % in the dry season (May to September). During the rainy season (December to March), there was an increase of approximately 5 %. These results showed that the most significant changes were observed in the dry season. According to Yin et al. (2013) this underestimation of precipitation in the dry season by the models could be explained by the fact that the models overestimate the convection in the Intertropical Convergence Zone (ITCZ) region, which in turn, could increase the subsidence and divergence of moisture on Amazon contributing to a dry bias in the dry season.

Figure 6 shows the percentage bias of moisture convergence (Eq. 6) in the dry (JJA, gray bar) and rainy season (DJF, white bar) from 1979 to 2005. For the purpose of analysis, values that exceed ±100 % were truncated. In general, there is underestimation by most models in the dry season, with the exception of box 4, which shows no predominance to neither overestimate nor underestimate moisture convergence. For this box it is shown that 11 of the 21 models show overestimation that exceeds 100 %. In all cases analyzed, box 3 shows the largest underestimates compared to observed data, exceeding 100 %. In this box, about 19 of the 21 models exceed −100 %. On average, the dry season underestimation is 27 %, while in the rainy season it is −16 %.

The mean SEM of four boxes is 11.3 mm day^{-1} during the dry season compared with 9.0 mm day^{-1} during the rainy season, emphasizing again that the largest error is found in the dry period due to larger underestimations. According to Satyamurty et al. (2013) drier conditions as observed in Fig. 4 are associated with reduction in moisture convergence over the forest. The spatial maps of moisture convergence at 850 hPa show that most models are dominated by a pattern of divergence of moisture in the dry season (JJA) in the four boxes analyzed.

On the other hand, observing the bias of this variable (Fig. 6) it is noticeable that the models are able to reproduce the spatial pattern of moisture convergence, but they fail to represent (underestimate) properly the observed value of the ERAI. During the rainy

season, these maps show predominance of moisture convergence in the region, but the bias of moisture convergence of four boxes shows a pattern of underestimation, similar to the situation in the dry season.

4 Discussion

To analyze the possible causes for the underestimation of model simulated precipitation in Amazonia and discuss the consequences for the analysis of future projections, it is interesting to explore to what extent the variability of rainfall is related to the SST in the surrounding oceans, and discuss how the models represent these processes.

4.1 Correlation between precipitation in the Amazon and SST in the adjacent oceans

The correlation between SST of the Pacific and Atlantic oceans and precipitation within the ensemble of 21 models as well as the interannual variability of rainfall in the Amazon between 1979 and 2005 is shown in Figs. 7 and 8 for the box 1, 2, 3 and 4 of Fig. 1.

In Fig. 7 (SST_MAY x PREC_JJA) we note that rainfall in northern Amazonia is correlated with the Atlantic and the Pacific SST. The figure shows that SST modulates the simulated rainfall in this region, in contrast with boxes 3 and 4, which show weaker correlations with no statistical significance. In addition, there is a dipole in the tropical Atlantic (Fig. 7a and d) with warmer SST in the North Atlantic and colder in the South Atlantic. The configuration of this inter-hemispheric gradient induces the positioning further north of the ITCZ and in general contributes to drier conditions over the Amazon.

The tropical Pacific includes the ENSO variability, which impacts precipitation in northeast Amazon region (Fig. 7d). The correlation in the tropical Atlantic Ocean suggests that SST here plays an important role in determining the interannual variability of rainfall in Amazonia, particularly in the dry season (Yoon and Zeng, 2010).

On the other hand, during the summer (Fig. 8) it appears that the tropical Pacific Ocean SST has more influence on rainfall over the Amazon than in winter. However, we note that the major influences of SST occur in eastern/northeastern Amazon (Fig. 8c and d) which show the strongest and most significant correlations. Based on the spatial pattern of SST in this period, we note that there is an ENSO-like pattern with greater intensity than observed in winter (Fig. 7). It is well known that variations of SST in the Pacific Ocean cause changes in precipitation in the Amazon (Ropelewski and Halper, 1987; Zeng, 1999). The influence of Atlantic SST is the main forcing for extreme events (droughts or floods) Amazon (Moura and Shukla, 1981; Liebmann and Marengo, 2001) that can impact the overall pattern of atmospheric circulation and moisture transport (Fu et al., 1999; Wang and Fu, 2002).

The positive bias in SST in most models shows that they overestimate the SST in the tropical Atlantic and Pacific Oceans. This pattern of the models can be responsible for drier conditions and reduced moisture convergence over the Amazon, since the observed values are generally above average on these oceans favoring large scale subsidence in the region, suppressing precipitation.

The correlation between SST and precipitation over Amazon (Fig. 9) provides us with a more quantitative view of how the SST is related to precipitation of the Amazon. In Fig. 9a–d (NAT) in JJA we note negative correlation of SST with rainfall in the Amazon (Good et al., 2008). Most models follow however the pattern of observed data from GPCP (black bar) and CMAP (bar red). The negative correlation is explained by the fact that the SST in May is relatively warmer, and JJA corresponds to the dry season in the Amazon which causes upward movement in regions of warm SST resulting in subsidence over the Amazon (Zeng et al., 2008). Moreover, during DJF (Fig. 9e–h, NAT) there is a positive correlation different from JJA. In this case, the SST is relatively cold, and at the same time, Amazon is on the edge of two main rainfall producing systems known as the Intertropical Convergence Zone (ITCZ) and South Atlantic Convergence Zone (SACZ). In general, the models reproduce the observational pattern observed for the four boxes studied suggesting that the models are able to capture this variability.

4.2 Bias of water balance in the present climate and possible causes for underestimation of modeled precipitation in Amazonia

The bias (Fig. 10) corresponds to the difference between the model and observation (ERAI) of vertically integrated moisture flux (Fig. 1, gray box). The left (right) refers to the JJA (DJF). The unit of the lateral flux is 10^7 kg s^{-1}, while the balance (convergence) is expressed in mm day^{-1}.

Evaluating the flow that enters the northern edge for both JJA and DJF (Fig. 10a and f, respectively), there is a positive bias that represents an overestimation of the models. It is known that the inflow in JJA is from the South Atlantic Subtropical High (ASAS), while in DJF, the entry is via trade winds from the northeast and ASAS. On the southern edge (Fig. 10b and g), the bias is positive indicating that the models overestimate the flow relative to ERAI. Some models underestimate this flow, for example, ACCES1-0, HADGEM2-CC and HADGEM2-ES during JJA. In DJF, most models have underestimated compared to ERAI.

On the southern border, the intensity of overestimation of the models is greater during JJA than DJF. However, the humidity output is greater in DJF than JJA. On the eastern edge (Fig. 10c and h), a negative bias is observed which indicates underestimation of the models, and this feature is seen in most of them in JJA, while in DJF, most models overestimate compared to the observed data. The reduction of moisture in JJA by the eastern edge shown by the models is dangerous for the maintenance and operation of the forest, since the moisture that enters through east edges of the domain is influenced by the South Atlantic Subtropical High (Satyamurty et al., 2013).

The western edge (Fig. 10d and i) is characterized by negative bias corresponding to underestimation in JJA and DJF, in other words, the models are simulating the output of humidity less intensely. The resulting balance of all flows shows a difference between JJA (Fig. 10e) and DJF (Fig. 10j).

During JJA most models underestimate the convergence, while in DJF we note overestimation. This difference is due to the fact that in JJA (Fig. 10c) the eastern flow

shows greater underestimation compared to DJF (Fig. 10f). Note also that the flow west is more underestimated in JJA (Fig. 10d) than DJF (Fig. 10i) which may have contributed to the underestimation seen in JJA (Fig. 10e) compared to DJF (Fig. 10j). In general, the moisture convergence in the Amazon is positive, that is, it is a source of atmospheric moisture in JJA and DJF (Satyamurty et al., 2013).

Joetzjer et al. (2013) compared simulations of precipitation in the Amazon during the climates of the present and the future by 13 CMIP3 and CMIP5 models. The results showed that, despite the improvement in spatial resolution of the models in CMIP5, precipitation is still underestimated by most of them. The models tend to represent the SST warmer than normal in the eastern Pacific and Atlantic inhibiting cloud formation and, consequently, the formation of precipitation.

The results of the correlation (Fig. 9) between the time series of precipitation in the four boxes in Fig. 1 and the spatial pattern of SST in the oceans Pacific (NINO3.4) and North and South Atlantic during JJA and DJF showed that the models were able to represent the correlation pattern of the observed data. This shows the skill of the models to represent satisfactorily the relationship between SST and precipitation, though the latter variable remains underestimated by the models despite the improvement in spatial resolution compared to previous versions of CMIP5.

In Fig. 9i–p (SAT) on average, the correlations are positive in both DJF and JJA corroborating the results found by Yoon and Zeng (2010) and Liebman and Marengo (2001). The correlations of the NINO3.4 area with Amazon rainfall (Fig. 9q–x) show negative correlations for most models in the JJA and DJF. Studies like Yoon and Zeng (2010) showed that the variability of rainfall in the Amazon is associated with variations in SST in the Pacific, in particular associated with El Niño/Southern Oscillation (ENSO). Langenbrunner and Neelin (2013) used 15 models of the CMIP5 during DJF and they analyzed the correlation between the Southern Oscillation Index (SOI) in the NINO3.4 region with global precipitation of the CMAP. The results showed that there was a negative correlation in the region Amazon confirming the results found here. Ronchail et al. (2002) evaluated the relationship between precipitation in the Amazon

basin and the SST in the equatorial Pacific during JJA and DJF quarters. The results showed a negative correlation between these two variables that occurred due to the influence of SST both the Pacific and the Atlantic oceans. Liebman and Marengo (2001) analyzed the variability of the rainy season and rainfall in the Brazilian Amazon basin during JJA and DJF and found that precipitation is negatively correlated with SST in the NINO3.4 region.

The flow of moisture that enters the Amazon occurs by the influence of the South Atlantic Subtropical High as well as the trade winds. Depending on the time of year, moisture penetration occurs through the action of these two systems or just the influence of one of them. It was noted that in JJA moisture penetration is predominantly via South Atlantic Subtropical High, while in summer, occurs both as the influence of this system by the trade winds. This was observed by the values of flows that have entered at each edge of the field of Fig. 1 (gray box). For example, on the north edge the flow is strongest in DJF than in JJA.

On the other hand, in the eastern edge the moisture flow is more intense in JJA than in DJF. In JJA models overestimated flows in the northern and southern edges and underestimated the eastern and western edges as a result of flows entering and leaving the domain. It was noticed that models underestimated this final balance, showing that there was less net moisture entry this quarter. The results for DJF showed that the models overestimated in the north and the east and underestimated in the south and west. Less moisture leaving by edge through the south and west edges favored overestimated in the calculation of the final balance. In general, both in DJF and JJA the Amazon acted as a sink of moisture to the atmosphere despite the underestimation (overestimation) in JJA (DJF).

Most studies using the CMIP5 simulations (Joetzjer et al., 2013; Yin et al., 2013) evaluated the energy balance of the surface, precipitation variability, fields associated with atmospheric circulation to understand why the models are deficient in satisfactorily representing the precipitation regimes over the Amazon. We aimed to contribute to this analysis by investigating the properties of moisture transport to Amazon.

The diagram in Fig. 11 shows a summary of the main results obtained from the analysis of the bias of precipitation and moisture convergence for the austral summer (DJF, Fig. 11a) and austral winter (JJA, Fig. 11b). During the wet season (DJF), our results show that the climate models have higher biases in rainfall simulation in the Northeastern region of Amazonia, while a lower bias and relatively better performance is noted in the Southwest. During the dry season (JJA), an opposite pattern is observed, that is, higher bias in rainfall simulations, probably related to higher bias of moisture convergence in the Southwest, and lower biases in the Northeast.

During DJF, the variability of SST in the Pacific is the main responsible for the modulation of atmospheric circulation and moisture convergence in Northeastern Amazonia (Fig. 8c and d). In this case, improvement in the model representations of the SST patterns and rainfall generating processes is clearly needed.

It is also noted that a positive bias of vertical motion (Fig. 5b) in the Southwestern part of the basin may, in this case, be responsible for a "better" performance of the models. However, this may be a case of unwittingly getting the right answer, where the models seem to show a good representation of the rainfall but wrongly represents its underlying processes.

In JJA, the higher bias obtained in the Southwest is less related to SST variability, but largely related to a bias in moisture convergence (Fig. 6). Because there is little relation to SST variability, it is likely that this underestimate of precipitation is caused by an underestimate of moisture recycling processes in the models.

In the Northeast, a lower bias was obtained, and, giving the high correlation of rainfall variability in this region with the patterns of SST in the Atlantic and Pacific (Fig. 7), it appears that the model simulations are representing relatively well the rainfall generation processes and teleconnections in this region in the dry season.

The results also show that some models such as HADGEM2, for example, showed a positive bias of precipitation in summer, which, particularly in the case of this model, can be attributed to perhaps the improvement in the representation of the generation of precipitation systems in the Amazon. Besides HADGEM2 models, other models show-

ing positive bias are: GISS-E2-R, INM-CM4. However, most models evaluated follow a trend for negative bias both for summer and for winter. Yin et al. (2013) used simulations of 11 models of CMIP5 to check whether precipitation is still underestimated on Amazon. The results showed that most models overestimate the Intertropical Convergence Zone (ITCZ) in the Atlantic or Eastern Pacific. This overestimation may intensify subsidence and moisture divergence on the Amazon, which contributes to a dry bias during the dry season.

Andreoli et al. (2012) showed by technique of composite using data observed in the rainy season (JFMA) that the presence of positive anomalies of Sea Level Pressure of the Equatorial Atlantic tend to weaken the Intertropical Convergence Zone (ITCZ) and that anomalies of positive SST in the eastern Pacific (upward movement over this region and subsidence over the Amazon) contributed to the suppression of convection, and subsequently the reduction of precipitation over Amazonia. In general, the poor representation of the SST in the Pacific and the Atlantic over the models can be a possible cause of underestimation of precipitation. Proper representation of these mechanisms is important because precipitation is a key factor in the hydrological cycle as well as for the carbon balance in the region.

5 Conclusions

We evaluated the performance of 21 models of CMIP5 on Amazon during the historical period that corresponds to the current climate (1979–2005) related to seasonality (DJF and JJA) of the moisture flux and precipitation by comparing the outputs of these models with the products of precipitation the GPCP and CMAP, SST (NOAA) as well as reanalysis ERAI.

The results showed that for the four boxes used to evaluate the models in subregions within Amazonia, most models underestimated the rainfall in JJA and DJF seasons. A possible explanation for the underestimation is the inadequate representation of precipitation-producing systems in the Amazon and the difficulty of models to repre-

sent satisfactorily the variability of SST in the Equatorial Pacific and Atlantic Oceans. SST is responsible for controlling precipitation particularly in the dry season.

For all subregions, model simulations of rainfall are biased, compared to the observations, but model performances vary from region to region. In general, higher biases are obtained in the Northeastern part of the basin during the DJF quarter (austral summer, wet season) and lower in the Southwest. During the JJA quarter (austral winter, dry season), the pattern is opposite: higher biases are obtained in the Southwestern and lower in the Northeast.

During DJF, rainfall variability in Amazonia is highly correlated with the SST patterns in the Atlantic and Pacific oceans, and this modulates the general circulation and moisture convergence in the region. During JJA, on the other hand, biases in model simulations are less likely to be related to SST variability, but special focus should be given to moisture recycling processes in the models.

The Supplement related to this article is available online at doi:10.5194/hessd-12-671-2015-supplement.

Acknowledgements. The authors acknowledge the project FP7-AMAZALERT (project number 282664) for financial support the development of the research. A. J. Dolman acknowledges support from a Ciência Sem Fronteiras "Pesquisador Visitante Especial" scholarship.

References

Aceituno, P.: On the functioning of the Southern Oscillation in the South American sector. Part I: Surface climate, Mon. Weather Rev., 116, 505–524, 1988.

Andreoli, R. V., Sousa, R. A. F., Kayano, M. T., and Candido, L. A.: Seasonal anomalous rainfall in the central and eastern Amazon and associated anomalous oceanic and atmospheric patterns, Int. J. Climatol., 32, 1193–1205, 2012.

Cook, B., Zeng, N., and Yoon, J. H.: Will Amazonia dry out? Magnitude and causes of change from IPCC climate model projections, Earth Interact., 16, 1–27, 2012.

Dee, D. P., Uppala, S. M., Simmons, A. J., Berrisford, P., Poli, P., Kobayashi. S., Andrae, U., Balmaseda, M. A., Balsamo, G., Bauer, P., Bechtold, P., Beljaars, A. C. M., van de Berg, L., Bidlot, J., Bormann, N., Delsol, C., Dragani, R., Fuentes, M., Geer, A. J., Haimberger, L., Healy, S. B., Hersbach, H., Hólm, E. V., Isaksen, L., Kallberg, P., Köhler, M., Matricardi, M., McNally, A. P., Monge-Sanz, B. M., Morcrette, J.-J., Park, B.-K., Peubey, C., de Rosnay, P., Tavolato, C., Thépaut, J.-N., and Vitart, F.: The ERA-interim reanalysis: configuration and performance of the data assimilation system, Q. J. Roy. Meteor. Soc., 137, 553–597, 2011.

Foley, J. A., Botta, A., Coe, M. T., and Costa, M. H.: El Niño–Southern oscillation and the climate, ecosystems and rivers of Amazonia, Global Biogeochem. Cy., 16, 1132, doi:10.1029/2002GB001872, 2002.

Fu, R., Zhu, B. and Dickinson, R. E.: How do atmosphere and land surface influence seasonal changes in the tropical Amazon?, J. Climate, 12, 1306–1321, 1999.

Good, P., Lowe, J. A., Collins, M., and Moufouma-Okia, W.: An objective tropical Atlantic sea surface temperature gradient index for studies of south Amazon dry-season climate variability and change, Philos. T. R. Soc. B., 363, 1761–1766, 2008.

Harris, P. P., Huntingford, C., and Cox, P. M.: Amazon basin climate under global warming: the role of the sea surface temperature, Philos. T. R. Soc. B., 363, 1753–1759, 2008.

Huffman, G. J., Adler, R. F., Arkin, P., Chang, A., Ferraro, R., Gruber, A., Janowiak, J., McNab, A., Rudolf, B., and Schneider, U.: The global precipitation climatology project (GPCP) combined precipitation dataset, B. Am. Meteorol. Soc., 78, 5–20, 1997.

Joetzjer, E., Douville, H., Delire, C., and Ciais, P.: Present-day and future Amazonian precipitation in global climate models: CMIP5 versus CMIP3, Clim. Dynam., 41, 2921–2936, 2013.

Kousky, V. E., Cavalcanti, I. F. A., and Kayano, M. T.: A review of the Southern Oscillation: oceanic–atmospheric circulation changes and related rainfall anomalies, Tellus A, 36, 490–504, 1984.

Langenbrunner, B. and Neelin, J. D.: Analyzing ENSO teleconnections in CMIP models as a measure of model fidelity in simulating precipitation, J. Climate, 26, 4431–4446, 2013.

Liebmann, B. and Marengo, J. A.: Interannual variability of the Rainy Season and Rainfall in the Brazilian Amazon Basin, J. Climate, 14, 4308–4318, 2001.

Lima, K. C., Satyamurty, P., and Fernandez, J. P. R.: Large-scale atmospheric conditions associated with heavy rainfall episodes in Southeast Brazil, Theor. Appl. Climatol., 101, 121–135, 2010.

Lorenz, C. and Kunstmann, H.: The hydrological cycle in three state-of-the-art reanalyses: intercomparison and performance analysis, J. Hydrometeorol., 13, 1397–1420, 2012.

Marengo, J. A., Tomasella, J., Alves, L. M., Soares, W., and Rodriguez, D. A.: The drought of 2010 in the context of historical droughts in the Amazon region, Geophys. Res. Lett., 38, L12703, doi:10.1029/2011GL047436, 2011.

Marengo, J. A., Tomasella, J., Alves, L. M., Soares, W., and Nobre, C. A.: Extreme climatic events in the Amazon basin: climatological and hydrological context of recent floods, Theor. Appl. Climatol., 107, 73–85, 2012.

Moura, A. D. and Shukla, J.: On the dynamics of droughts in northeast Brazil: observations, theory and numerical experiments with a general circulation model, J. Atmos. Sci., 38, 2653–2675, 1981.

Mueller, B., Hirschi, M., Jimenez, C., Ciais, P., Dirmeyer, P. A., Dolman, A. J., Fisher, J. B., Jung, M., Ludwig, F., Maignan, F., Miralles, D. G., McCabe, M. F., Reichstein, M., Sheffield, J., Wang, K., Wood, E. F., Zhang, Y., and Seneviratne, S. I.: Benchmark products for land evapotranspiration: LandFlux-EVAL multi-data set synthesis, Hydrol. Earth Syst. Sci., 17, 3707–3720, doi:10.5194/hess-17-3707-2013, 2013.

Pinto, L. I., Costa, M. H., Lima, F. Z. L., Diniz, L. M. F., Sediyama, G. C., and Pruski, F. F.: Comparação de produtos de precipitação para a América do Sul, Rev. Bras. Met., 24, 461–472, 2009.

Rao, V. B., Cavalcanti, I. F. A., and Hada, K.: Annual variation of rainfall over Brazil and water vapor characteristics over South America, J. Geophys. Res., 101, 26539–26551, 1996.

Ronchail, J., Gerard, C., Molinier, M., Guyot, J. P., Chaves, A. G. M., Guimaraes, V., and Oliveira, E.: Interannual rainfall variability in the Amazon Basin and sea–surface temperatures in the Equatorial Pacific and the Tropical Atlantic Oceans, Int. J. Climatol., 22, 1663–1686, 2002.

Ropelewski, C. F. and Halpert, M. S.: Global and regional scale precipitation associated with El Niño/Southern Oscillation, Mon. Weather Rev., 115, 1606–1626, 1987.

Satyamurty, P., Costa, C. P. W., and Manzi, A. O.: Moisture source for the Amazon Basin: a study of contrasting years, Theor. Appl. Climatol., 111, 195–209, 2013.

Smith, T. M., Reynolds, R. W., Peterson, T. C., and Lawrimore, J.: Improvements to NOAA's historical merged land–ocean surface temperature analysis (1880–2006), J. Climate, 21, 2283–2296, 2008.

Taylor, K. E., Ronald, J. S., and Gerald, A. M.: An overview of CMIP5 and the experiment design, B. Am. Meteorol. Soc., 93, 485–498, 2012.

Wang, H. and Fu, R.: Cross-equatorial flow and seasonal cycle of precipitation over South America, J. Climate, 15,1591–1608, 2002.

Xie, P. and Arkin, P. A.: Global precipitation: a 17-year monthly analysis based on Gauge observations, satellite estimates, and numerical model outputs, B. Am. Meteorol. Soc., 78, 2539–2558, 1997.

Xie, S. P. and Carton, J. A.: Tropical Atlantic variability: patterns, mechanisms, and impacts, Earth climate: the Ocean–Atmosphere Interaction, Geoph. Monog. Series, 147, 121–142, 2004.

Yin, L., Fu, R., Shevliakova, E., and Dickson, R. E.: How well can CMIP5 simulate precipitation and its controlling processes over tropical South America?, Clim. Dynam., 41, 3127–3143, 2013.

Yoon, J. H. and Zeng, N.: An Atlantic influence on Amazon rainfall, Clim. Dynam., 34, 249–264, 2010.

Zeng, N.: Seasonal cycle and interannual variability in the Amazon hydrologic cycle, J. Geophys. Res., 104, 9097–9106, 1999.

Zeng, N., Yoon, J. H., Marengo, J. A., Subramaniam, A., Nobre, C. A., Mariotti, A., and Neelin, J. D.: Causes and impacts of the 2005 Amazon drought, Environ. Res. Lett., 3, 1–9, 2008.

Table 1. The WCRP CMIP5 models used in this study.

	Model	Expansion	Source	Atmospheric Resolution
1	ACCESS1.0	Australian Community Climate and Earth-System Simulator, version 1.0	Commonwealth Scientific and Industrial Research Organisation (CSIRO) and Bureau of Meteorology, Australia	192 × 145
2	BCC-CSM1.1	Beijing Climate Center, Climate System Model, version 1.1	Beijing Climate Center, China	128 × 64
3	CanESM2	Second Generation Canadian Earth System Model	Canadian Centre for Climate Modelling and Analysis, Canada	128 × 64
4	CCSM4	Community Climate System Model, version 4	National Center for Atmospheric Research (NCAR), United States	288 × 192
5	CNRM-CM5	Centre National de Recherches Météorologiques Coupled Global Climate Model, version 5	Centre National de Recherches Meteorologiques/Centre Europeen de Recherche et Formation Avancées en Calcul Scientifique, France	256 × 128
6	CSIRO Mk3.6.0	Commonwealth Scientific and Industrial Research Organisation Mark, version 3.6.0	CSIRO and Queensland Climate Change Centre of Excellence, Australia	192 × 96
7	FGOALS-s2	Flexible Global Ocean–Atmosphere–Land System Model gridpoint, second spectral version	Institute of Atmospheric Physics, Chinese Academy of Sciences,China	128 × 108
8	GFDL-CM3	GFDL Climate Model, version 3 (GFDL-CM3)	National Oceanic and Atmospheric Administration (NOAA)/ GFDL, United States	144 × 90
9	GFDL-ESM2G	Geophysical Fluid Dynamics Laboratory Earth System Model with Generalized Ocean Layer Dynamics (GOLD) component (ESM2G)	National Oceanic and Atmospheric Administration (NOAA)/ GFDL, United States	144 × 90
10	GFDL-ESM2M	Geophysical Fluid Dynamics Laboratory Earth System Model with Modular Ocean Model 4 (MOM4) component (ESM2M)	NOAA/GFDL, United States	144 × 90
11	GISS-E2-R	Goddard Institute for Space Studies Model E2, coupled with the Russell ocean model	NASA GISS, United States	144 × 90
12	HadGEM2-CC	Hadley Centre Global Environment Model, version 2–Carbon Cycle	Met Office, UK	192 × 145
13	HadGEM2-ES	Hadley Centre Global Environment Model, version 2–Earth System	Met Office, UK	192 × 145
14	INM-CM4.0	Institute of Numerical Mathematics Coupled Model, version 4.0	Institute of Numerical Mathematics, Russia	180 × 120
15	IPSL-CM5A-LR	L'Institut Pierre-Simon Laplace Coupled Model, version 5A, coupled with NEMO, low resolution	L'Institut Pierre-Simon Laplace, France	96 × 96
16	IPSL-CM5A-MR	L'Institut Pierre-Simon Laplace Coupled Model, version 5A, coupled with NEMO, mid resolution	L'Institut Pierre-Simon Laplace, France	96 × 96
17	MIROC5	Model for Interdisciplinary Research on Climate, version 5	Atmosphere and Ocean Research Institute (AORI) (The University of Tokyo), National Institute for Environmental Studies (NIES), and Japan Agency for Marine-Earth Science and Technology (JAMSTEC), Japan	256 × 224
18	MIROC-ESM	Model for Interdisciplinary Research on Climate, Earth System Model	AORI, NIES, and JAMSTEC, Japan	128 × 64
19	MPI-ESM-LR	Max Planck Institute Earth System Model, low resolution	Max Planck Institute for Meteorology, Germany	192 × 96
20	MRI-CGCM3	Meteorological Research Institute Coupled Atmosphere–Ocean General Circulation Model, version 3	Meteorological Research Institute, Japan	320 × 160
21	NorESM1-M	Norwegian Earth System Model, version 1(intermediate resolution)	Norwegian Climate Centre, Norway	144× 96

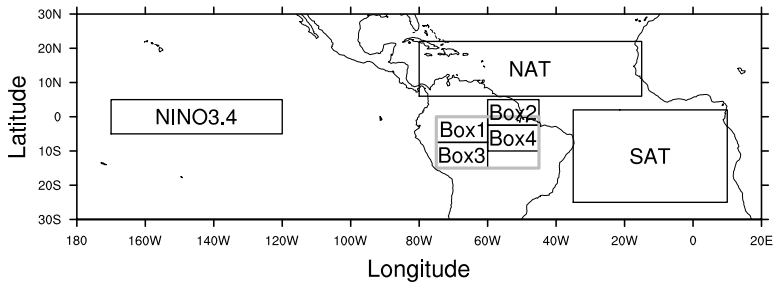

Figure 1. Study area. NAT is the region of the North Atlantic and SAT is the South Atlantic region. The gray box is used in the analysis of climatology (Fig. 2), Taylor diagram (Fig. 3) and discussion of biases in modeled water transport (Fig. 10).

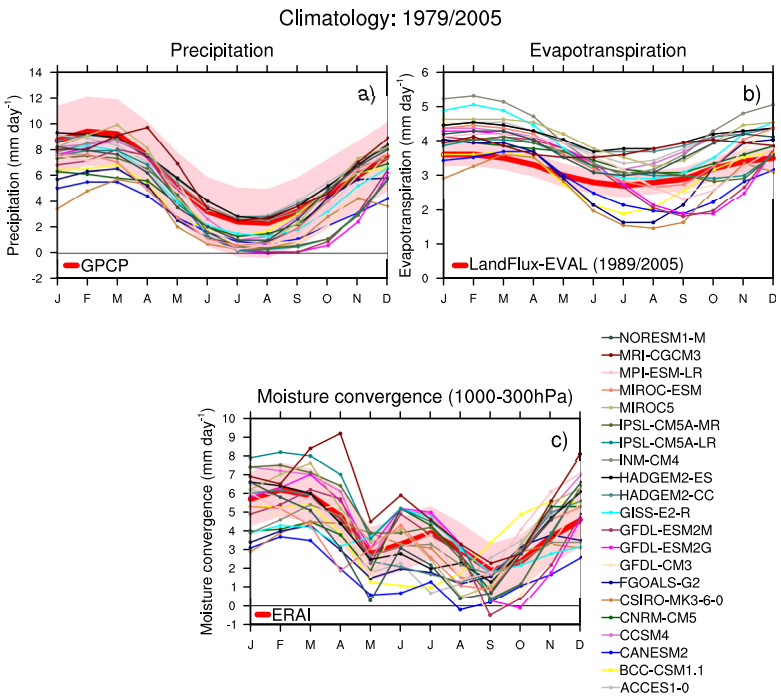

Figure 2. Climatology of Amazonian **(a)** precipitation (mm day^{-1}), **(b)** evapotranspiration (mm day^{-1}) and, **(c)** moisture convergence (mm day^{-1}) for the 1979–2005 period, and observed (red thick line) and simulated (colored thin lines) by the CMIP-5 suite of climate models. The shaded region represents the SD of the observation.

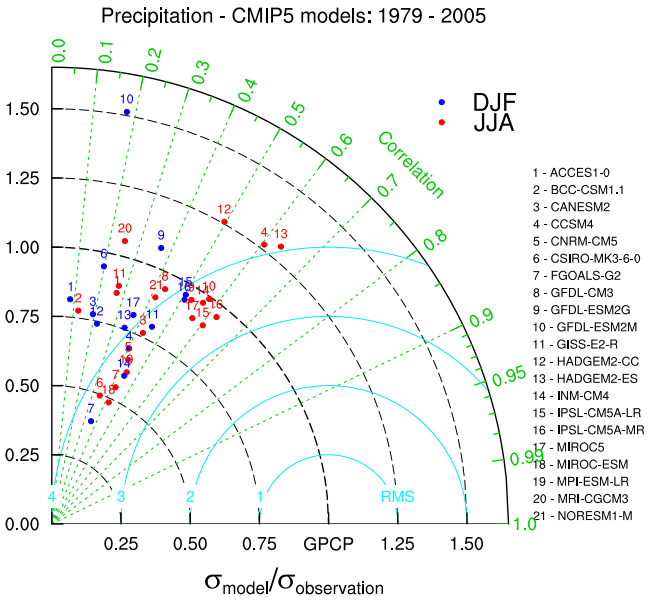

Figure 3. Taylor diagram for correlation (green line) and SD (black line) for precipitation during JJA and DJF (1979–2005) using GPCP like reference. On the Taylor diagram, angular axes show correlation between modeled and observed; radial axes show SD (root-mean-square deviation [cyan line]) normalized against that of observation. The domain used is the gray box of the Fig. 1. Only positive correlations are shown. The BCC-CSM1.1, CNRM-CM5, GFDL-CM3, MIROC-ESM, MPI-ESM-LR, MRI-CGCM3 and NORESM1-M models show negative correlations during DJF.

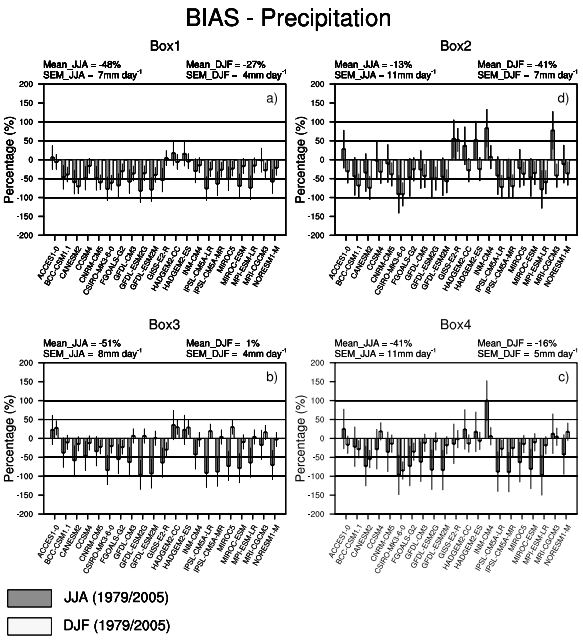

Figure 4. BIAS of precipitation in relation to rainfall from GPCP. The average (Mean) of each season as well as the standard error of the mean (SEM) are also shown in the upper left/right corner. The value of SEM is calculated as the ratio between the SD and square root the number of elements in the sample. SD is shown by the thin black bars.

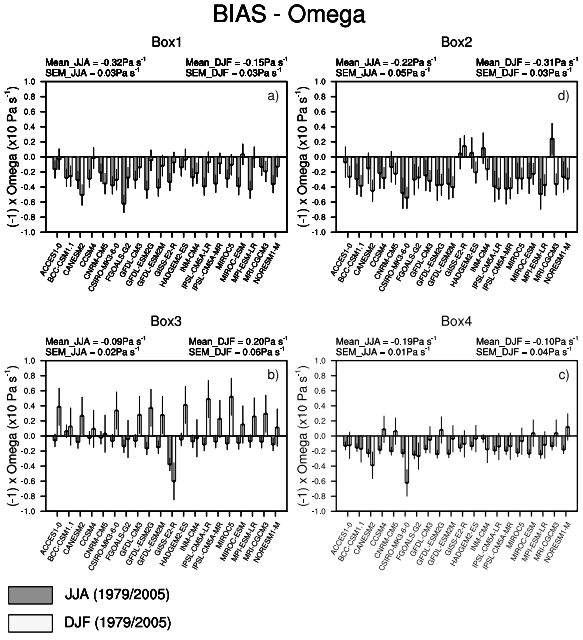

Figure 5. BIAS of Omega. The average (Mean) value of each season as well as the standard error of the mean (SEM) are shown in the upper left/right corner. The value of SEM is calculated as the ratio between the SD and the root square of the number of elements in the sample. SD is shown by the thin black bars. The values were multiply by −1 to show that models underestimate omega (ERAI). The HADGEM2-CC model does not provide any omega information.

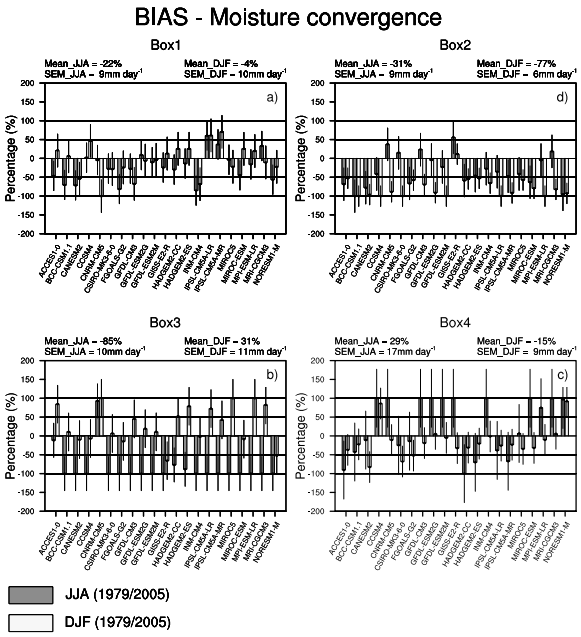

Figure 6. BIAS of moisture convergence in relation to ERAI. The average (Mean) of each season as well as the standard error of the mean (SEM) are also shown in the upper left/right corner. The value of SEM is calculated as the ratio between the SD and square root the number of elements in the sample. SD is shown by the thin black bars.

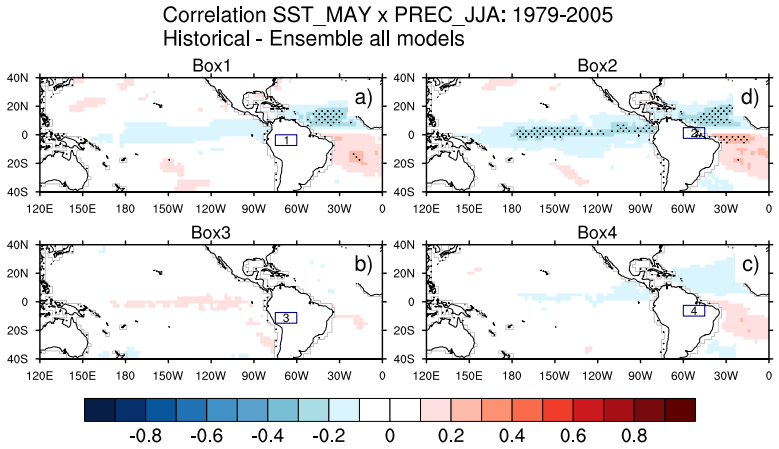

Figure 7. Ensemble correlation between SST_MAY and PREC_JJA of all 21 models of the CMIP5 to box 1, 2, 3 and 4. Dotted areas are significant at the 90 % level of significance.

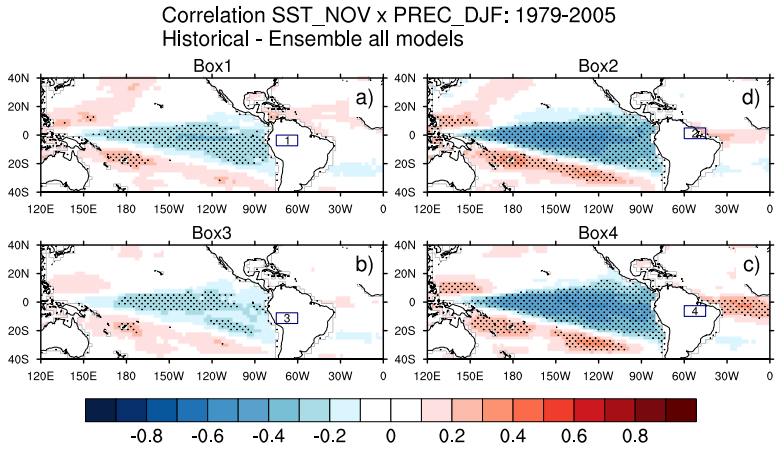

Figure 8. Ensemble correlation between SST_NOV and PREC_DJF of all 21 models of the CMIP5 to box 1, 2, 3 and 4. Dotted areas are significant at the 90 % level of significance.

Discussion Paper | Discussion Paper | Discussion Paper | Discussion Paper |

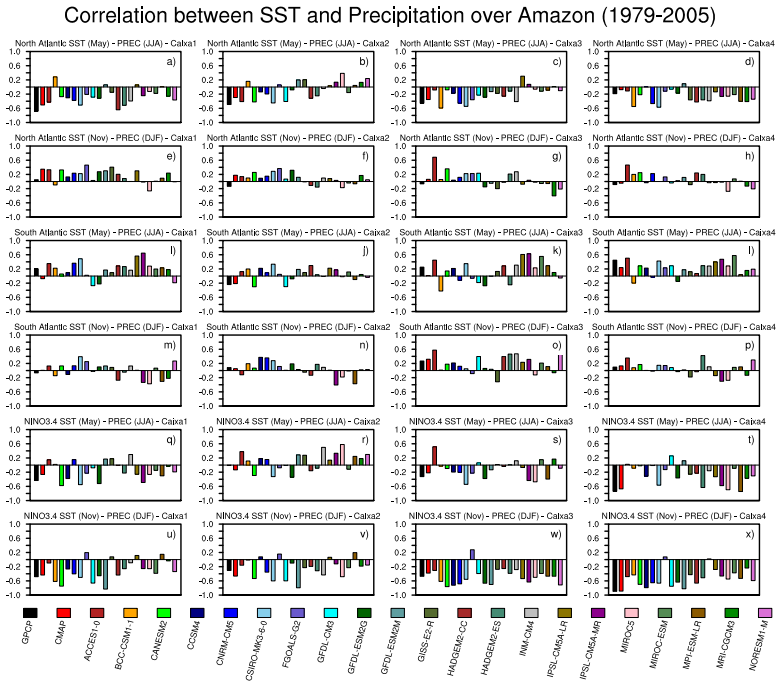

Figure 9. Correlation between regions of SST in the Pacific and Atlantic oceans and precipitation in the Amazon to box 1, 2, 3 and 4 (Fig. 1).

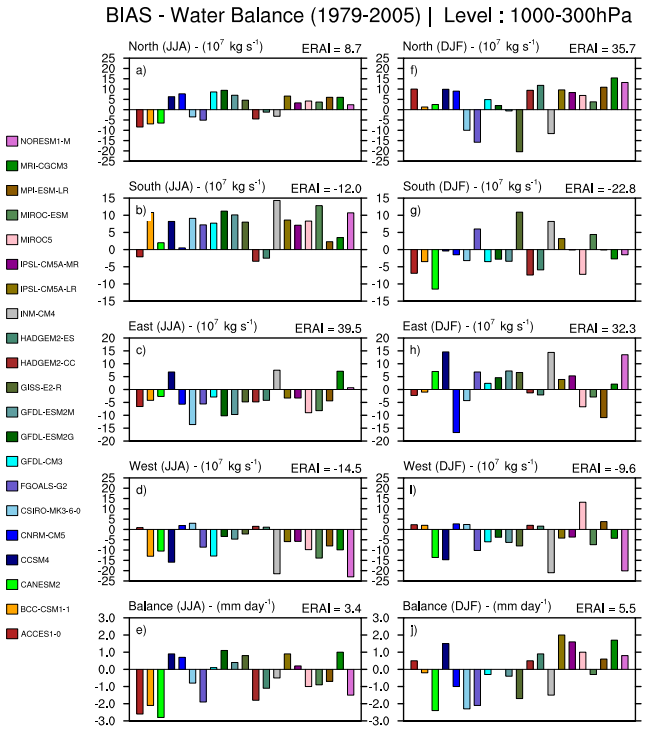

Figure 10. BIAS of the moisture flux by components in JJA (left) and DJF (right) period. The unit flows north, south, east and west are in $10^7\,kg\,s^{-1}$ and balance unit is $mm\,day^{-1}$. In the upper right corner of each figure is the calculated flow of moisture ERAI. The bars are the difference between the models and the ERAI. The moisture flux is calculated on the edges in the gray box in Fig. 1.

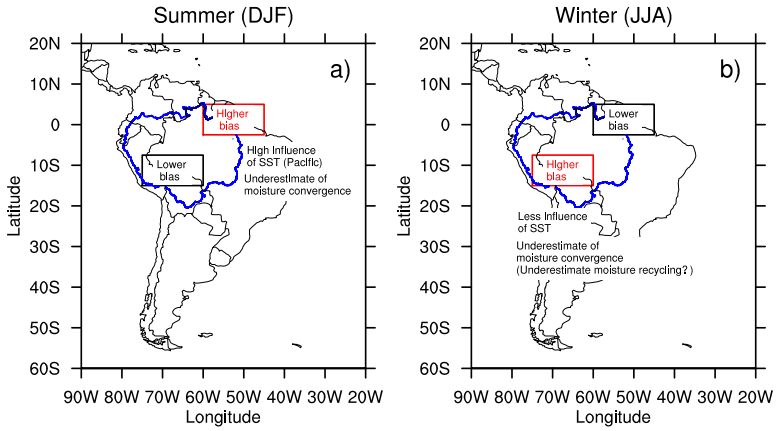

Figure 11. Schematic diagram showing the bias of precipitation and moisture convergence. The blue outline represents the Amazon basin.

Discussion Paper | Discussion Paper | Discussion Paper | Discussion Paper |